Electronic Supplementary Material (ESI) for Sustainable Energy & Fuels.

Rapid formation of self-organised Ag nanosheets with high efficiency and selectivity in CO_2 electroreduction to CO

Chong-Yong Lee,*[a] Yong Zhao,[a] Caiyun Wang,[a] David R. G. Mitchell[b] and Gordon G. Wallace*[a]

[a]ARC Centre of Excellence for Electromaterials Science, Intelligent Polymer Research Institute, AIIM, Innovation Campus, University of Wollongong, Wollongong, NSW 2500, Australia.

[b]Electron Microscopy Centre, AIIM, Innovation Campus, University of Wollongong, Wollongong, NSW 2500, Australia.

*** Corresponding authors**

E-mails: cylee@uow.edu.au (C.-Y.L), gwallace@uow.edu.au (G.G.W.)

Experimental section

Procedure

Chemicals and Materials

Silver foils (0.125 mm, 99.99 %, Advent Research Materials) were used as substrates. Prior to use, silver foils were cleaned via ultrasonication in ethanol, followed by rinsing with Milli-Q water (18 MΩ cm) water and drying the samples in a nitrogen stream. The chemicals ($NaHCO_3$, NaCl, ethanol, acetone) were purchased from ChemSupply and used as-received. Milli-Q water was used in all aqueous-based experiments.

Electrochemical experiments

Anodization

A potentiostat (CH Instrument 650D) was used for electrochemical experiments. For anodisation, a three-electrode configuration was employed with Ag foil as the anode, a platinum gauze as a counter electrode, and an Ag/AgCl (3M NaCl) as a reference electrode. After the anodisation process, the anodised samples were rinsed with Milli-Q water and then dried in a nitrogen stream.

CO_2 reduction

A two-compartment gastight glass H-cell was used for CO_2 electrochemical reduction. The cathodic and anodic compartments were separated by a Nafion membrane (Nafion® 117, Alfa- Aesar). Each compartment contained 30 mL of 0.5 M $NaHCO_3$ electrolyte. The volume of the headspace is approximately 20 mL. Prior to the CO_2 reduction, the working electrodes were reduced at a constant potential of -2.0 V (vs. Ag/AgCl 3 M NACl) for 5 min with a constant CO_2 (99.99%, BOC) flow at 20 mL min^{-1} to reduce the AgCl to Ag. The reduced Ag was the rinsed with Mili-Q water.

The H-cell was thoroughly cleaned with introduction of new 0.5 M $NaHCO_3$ electrolyte, with purging of CO_2 for 30 min, before the CO_2 reduction was carried out at different potentials. The electrolyte was magnetically stirred at 250 rpm to enhance the mass transport of CO_2. All the constant potential experiments were corrected using the automatic iR compensation function on the potentiostat, unless otherwise stated. The potentials were measured against the reference electrode and converted to the reversible hydrogen electrode (RHE) reference scale by the following equation, $E_{RHE} = E_{Ag/AgCl} + 0.21 + 0.0591pH$. The pH value of CO_2-saturated 0.5 M $NaHCO_3$ aqueous solution is 7.2. The current density reported in this work was normalised to the geometric surface area. The cyclic voltametric experiments were performed as the above configurations, but without iR correction.

Products analysis

During the electrolysis, CO_2 was continuously bubbled into the cathodic compartment at a rate of 20.0 mL min^{-1} controlled by a mass flow controller (GFC17, Aalborg®) and vented directly into the gas-sampling loop (1 mL) of a gas chromatograph (GC) (8610C, SRI Instruments).[1] The GC was equipped with a packed MolSieve 5A column and a packed Haysep D column. Argon was used as the carrier gas. A fame ionization detector (FID) with methan-izer was used to quantify CO, and a thermal conductivity detector (TCD) was used to quantify H_2. An external standard method was adopted with a standard gas mixture (BOC) composed of H_2, CO, CH_4, C_2H_4, C_2H_6 and CO_2. The first GC run was initiated at the 20^{th} min, and thereafter a measurement was taken three times, 16 min apart. The average of the results from these four measurements was used in the data analysis. Long term stability experiment was performed at extended hours with the analysis of the initial and last hour products.

Surface area measurement

The electrochemical surface area measurement was conducted in a three electrode cell using a Pt counter electrode and an Ag/AgCl reference electrode. The electrolyte was 0.1 M NaOH solution (N_2 saturated) with a pH of 12.6. After electrochemical reduction at -1.34 V vs. Ag/AgCl (i.e., -0.40 V vs. RHE) for 10 minutes, the electrodes were oxidised at 0.21 V vs. Ag/AgCl (i.e., 1.15 V vs. RHE), which was believed to form only a monolayer of Ag_2O or AgOH.[2] The relative chemical surface areas between different Ag electrodes were obtained by comparing the current passed during the oxidation process.

Structural characterization

The as-prepared AgCl, reduced Ag and Ag foil were analysed by X-ray diffraction (XRD, GBC MMA diffractometer) with Cu Kα radiation at a scan rate of 2 degree per min. The morphology of the samples was investigated by field emission scanning electron microscopy (FESEM, JEOL JSM-7500FA) and scanning transmission electron microscopy (STEM, JEOL ARM200F) in conjunction with energy-dispersive X-ray spectroscopy (EDS). X-ray photoelectron spectroscopy (XPS) was measured on a SPECS PHOIBOS 100 Analyser with X-ray excitation provided by Al Kα radiation ($h\nu$ = 1486.6 eV) at a voltage of 12 kV and a power of 120 W. The XPS binding energy spectra were recorded at a pass-energy of 20 eV in the fixed analyser transmission mode. All the spectra were calibrated by C 1s = 284.6 eV.

Table S1 Summary of the selected state-of-the-art Ag, Cu, Mo and Au CO_2 reduction electrocatalysts with a focus on their preparation time.

Materials	Synthesis approach	Required step and time	Morphology	Performance	Ref.
Ag	alloy-dealloying to form nanoporous Ag	alloy (12 h), 2 steps dealloy (15 min + 30 min), attachment of nanoporous Ag onto nickel wire (undefined)	nanoporous	overpotential = 0.39 V, FE_{CO} = 90 %	2
Ag	electrooxidation and electroreduction	anodisation (12 h) + electroreduction (30 min)	nanocorals	overpotential = 0.37 V, FE_{CO} = 95 %	3
Ag	electrooxidation and electroreduction	Ag oxide formation by applying square wave pulsed potential (5 h) + electroreduction (undefined)	porous-like nanostructure	overpotential = 0.49 V, FE_{CO} = 80 %	4
Ag	electrooxidation and electroreduction	anodisation (> 7h) + electroreduction (undefined)	porous	overpotential = 0.39 V, FE_{CO} = 85 %	5
Ag	electrodeposition into polystyrene host-template + template removal	polystyrene host-template (4-5 days) + electrodeposition (undefined) + removal of template (~ 12h)	inverse-opal	overpotential = 0.49 V, FE_{CO} = 90 % (based on film with roughness factor of 105)	6
Ag	electrooxidation and electroreduction	anodisation (90 s) + electroreduction (5 min)	nanosheets	overpotential = 0.29 V, FE_{CO} = 95 %	This work
Cu	annealing + electroreduction	best electrode annealed at 500^{o}C for 12 h + electroreduction	nanorods	overpotential = 0.19 to 0.39 V, FE_{CO} = 40 %	7
Mo	chemical vapour deposition (CVD) + sulphurization	CVD (undefined) +sulphurisation - heating to reach 200 ^{o}C (undefined), 30 min to reach 600 ^{o}C (kept for 15 min) + cooling down to room temperature (undefined)	vertically aligned nanoflakes	overpotential = 0.654 V, FE_{CO} = 98 % (in mixture of aqueous and ionic liquid solution).	8
Au	electrooxidation and electroreduction	require intensive pre-treatment = annealing of gold at 750^{o}C for 12 h + applying square-wave potential to form thick gold oxide (60 min) + electroreduction (15 min)	agglomerated nanoparticles	overpotential = 0.24 V, FE_{CO} = > 96 %	9

Table S2 The influence of electrolyte, anodisation voltage and duration, on the resulting morphology of the anodised layers.

Electrolyte / NaCl	Voltage / V	Time / s	Description
0.5 M	1.0	90	a layer with microchannels
1.0 M	1.0	90	a layer with microchannels and low density nanosheets
1.0 M	1.0	300	a thick layer with cracked surface
2.0 M	1.0	90	a layer with high density nanosheets
3.0 M	0.1	90	a layer with microchannels
3.0 M	0.3	90	a layer with medium density nanosheets
3.0 M	0.6	90	a layer with high density nanosheets
3.0 M	1.0	60	a layer with high density nanosheets, thickness of ~ 11 μm
3.0 M	1.0	90	a layer with high density nanosheets, thickness of ~ 16 μm
3.0 M	1.0	120	a layer with high density nanosheets, thickness of ~ 19 μm

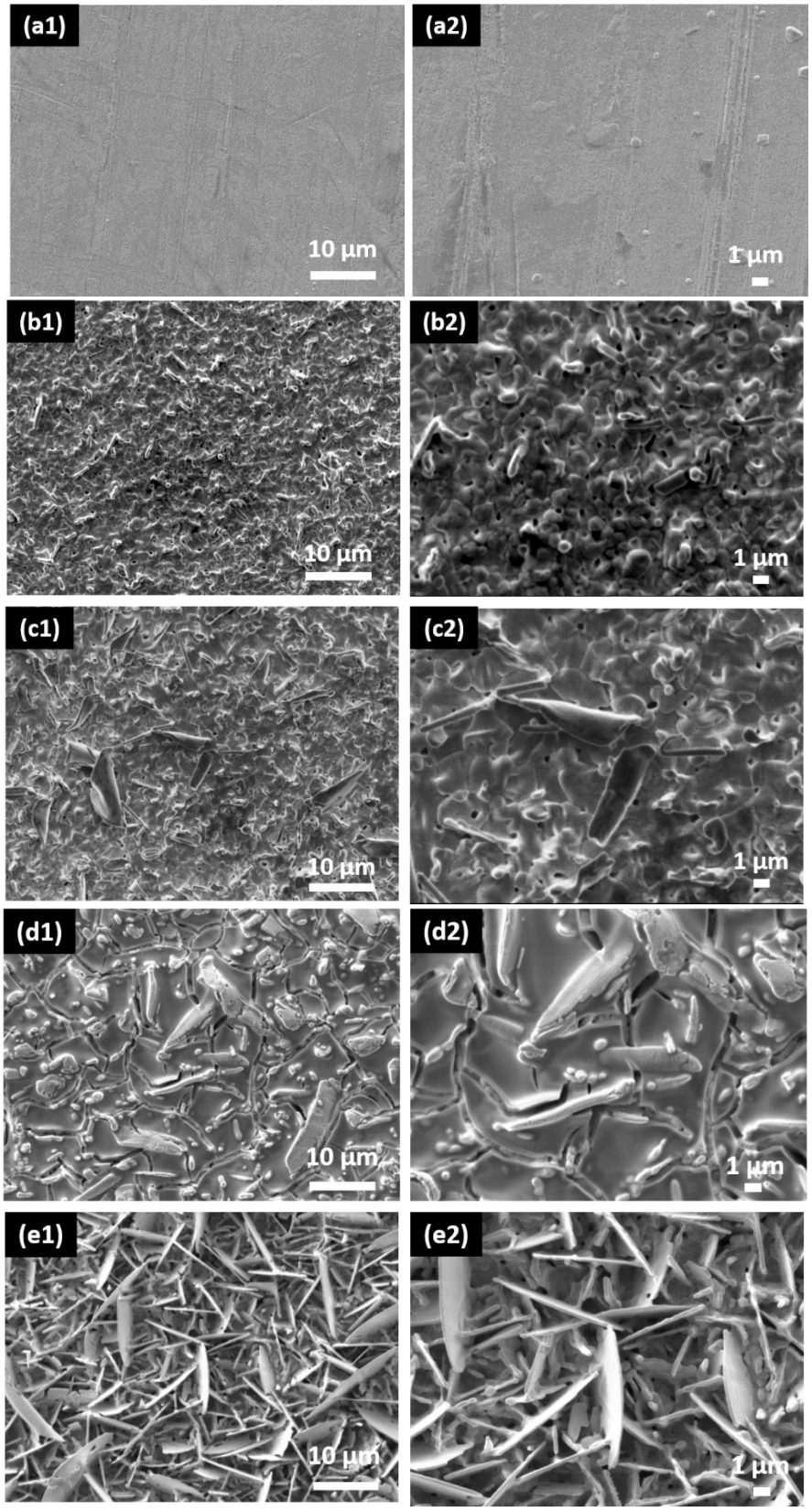

Figure S1 SEM images of a Ag foil (a1-a2), and AgCl layers formed by anodising Ag foils at 1.0 V for the times indicated using various NaCl concentrations: (b1-b2) 0.5 M, 90 s; (c1-c2) 1.0 M, 90 s; (d1-d2) 1.0 M, 300 s; (e1-e2) 2.0 M, 90 s.

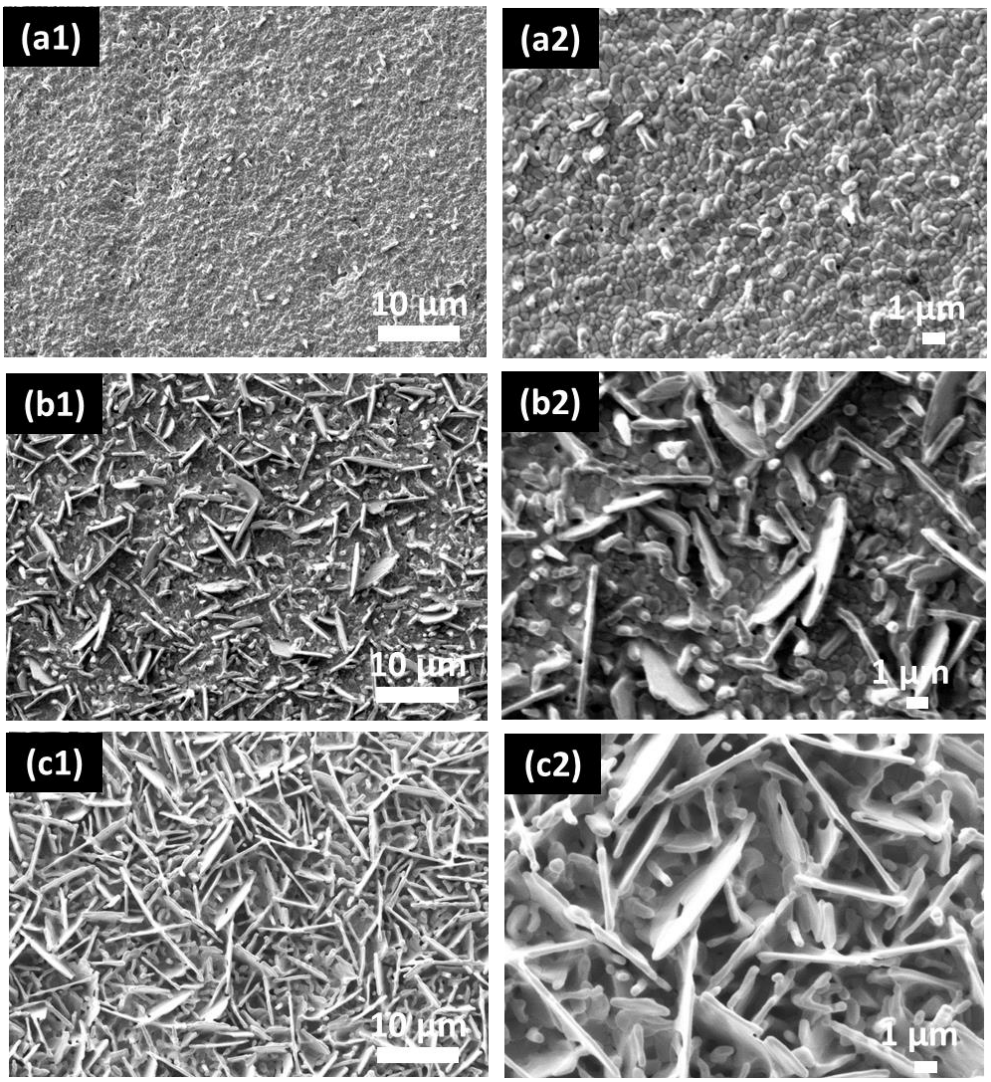

Figure S2 SEM images of AgCl layers formed by anodising Ag foils in 3.0 M NaCl for 90 s at an applied potential of: (a1-a2) 0.1 V; (b1-b2) 0.3 V; (c1-c2) 0.6 V.

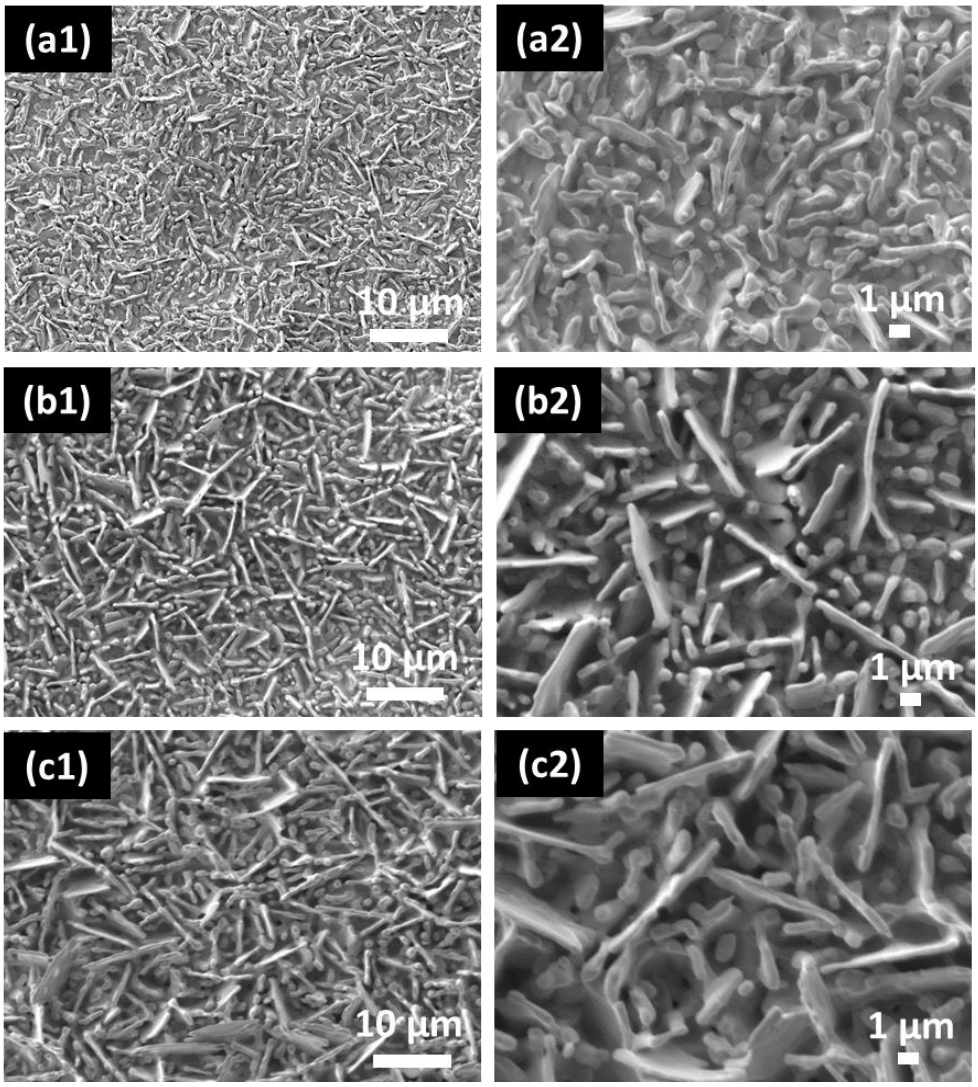

Figure S3 SEM images of AgCl layers formed by anodising Ag foils at 1.0 V in 3.0 M NaCl, with an anodisation duration of: (a1-a2) 10 s; (b1-b2) 30 s and (c1-c2) 60 s.

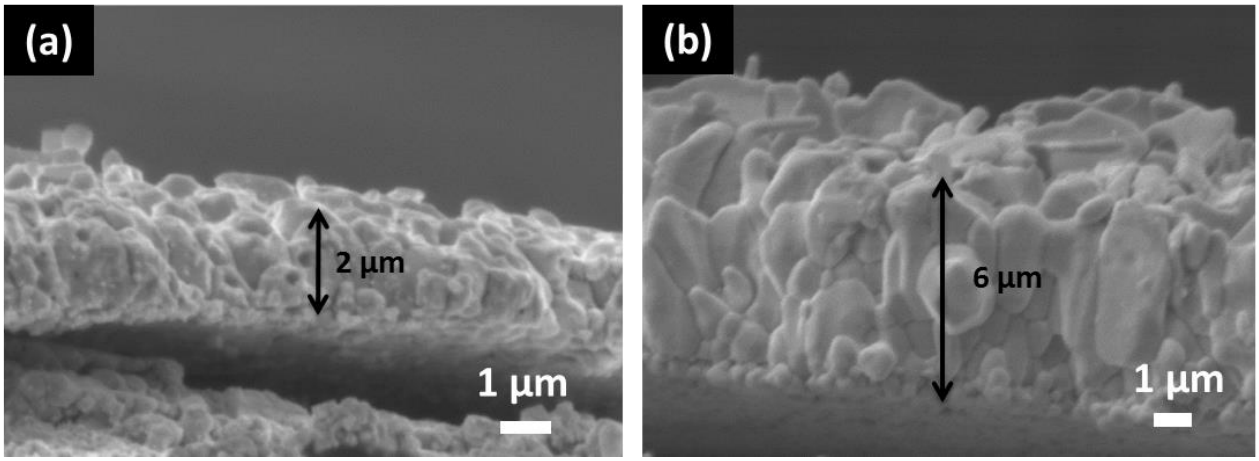

Figure S4 SEM cross-sectional images of AgCl layers formed by anodising Ag foil in 3.0 M NaCl for 90 s at 1.0 V for a) 10 s and b) 30 s.

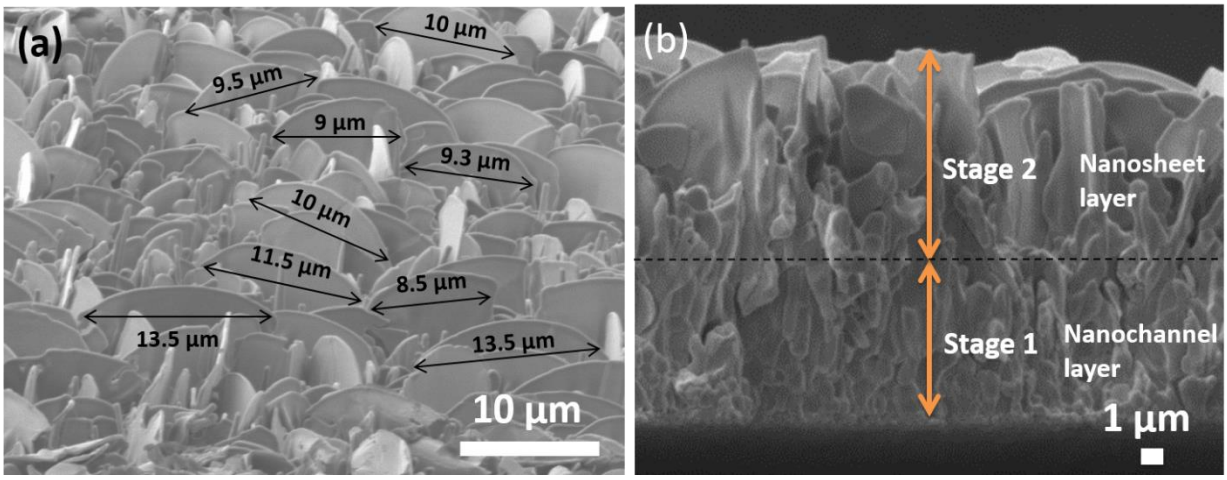

Figure S5 (a) A SEM image from a tilted specimen to get indication of nanosheet lateral sizes, (b) A SEM cross-sectional image of AgCl layers formed by anodising Ag foil in 3.0 M NaCl that showing the stages of anodic growth: stage 1 - formation of nanochannel layer, follow by stage 2 - formation of nanosheet layer.

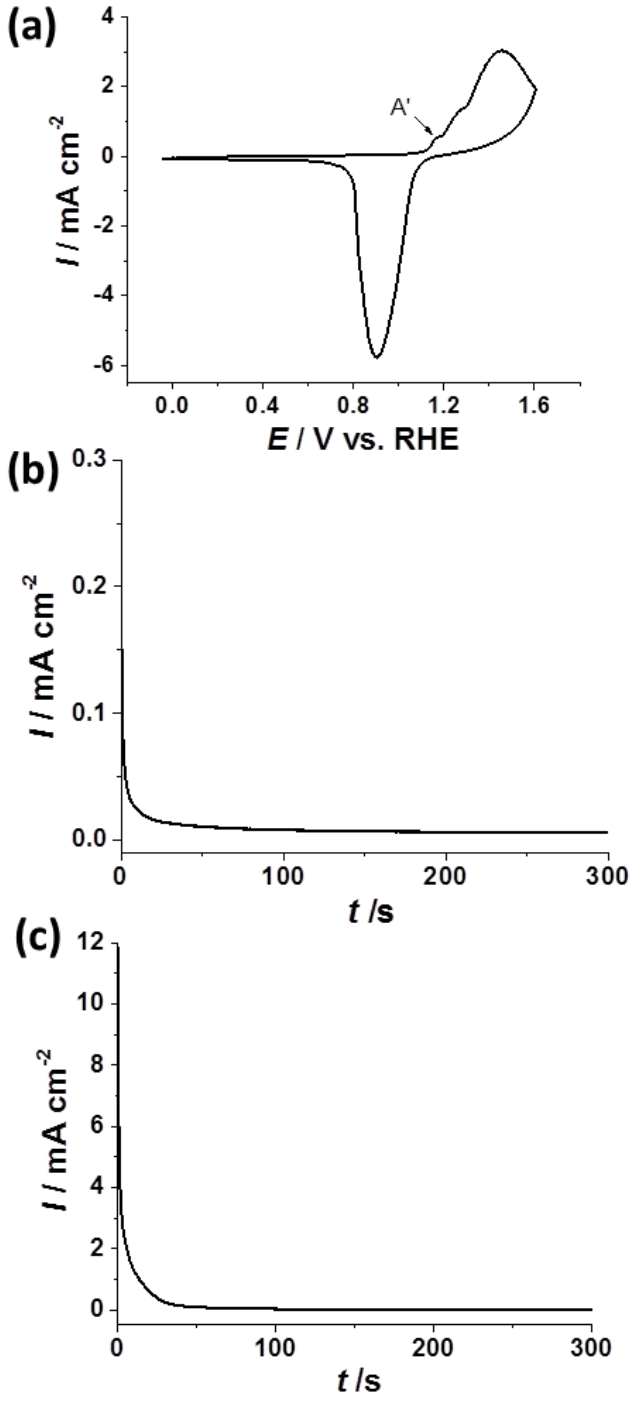

Figure S6 (a) A cyclic voltammogram of Ag in 0.1 M NaOH, under N_2 atmosphere at 100 mV s^{-1}. A' is a peak current attributed to Ag oxidation to form a monolayer of Ag_2O or AgOH. The current transient curves at 1.15V vs. RHE for (b) polycrystalline Ag, and (c) Ag nanosheets performed in 0.1 M NaOH and under N_2 atmosphere. The charge required to oxidise one monolayer of Ag nanosheet-based electrode (Q = 46.74 mC cm^{-2}) is approximately 17 times larger than polycrystalline Ag-based electrode (Q = 2.73 mC cm^{-2}).

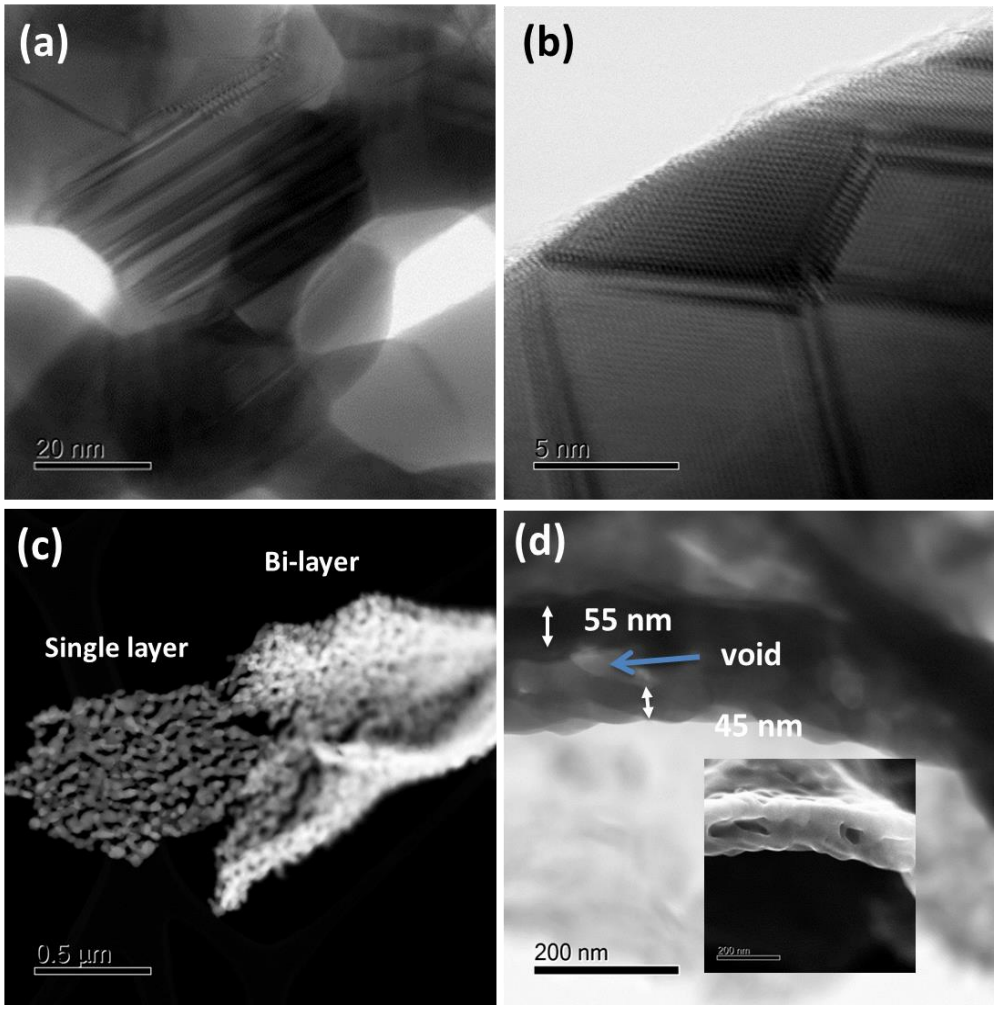

Figure S7 Representative STEM images of the reduced Ag nanosheet: (a) bright field image as shown in the Figure 3 of the main text; (b) bright field image showing intersecting twin boundaries resulting in regions of differing diffraction contrast; (c) high angle annular dark field (HAADF) image showing a flat single layer and curved bilayer structure (which curves up out of the plane of focus); (d) bright field image showing the porosity between the bi-layer of the reduced Ag nanosheets, inset shows the corresponding secondary electron (morphological) image highlighting the pores which break the surface at the edge of the sheet.

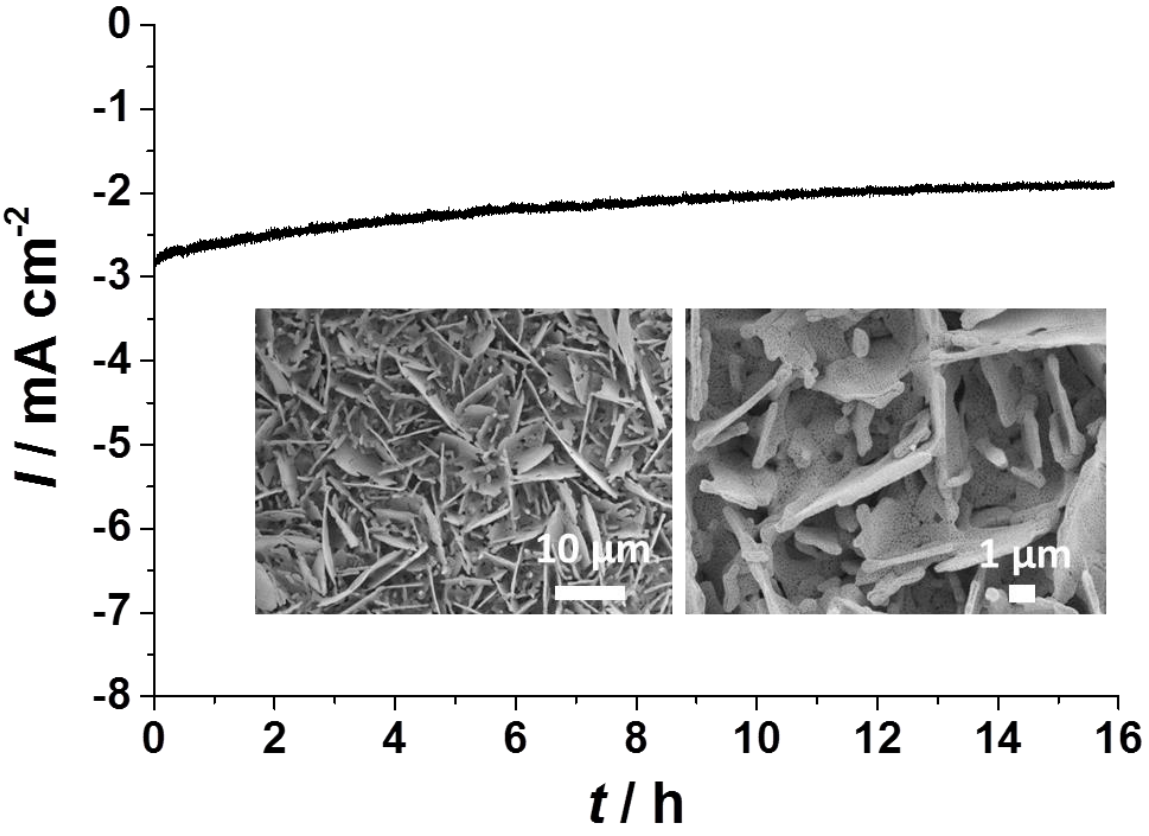

Figure S8 The current transient curve of an Ag nanosheet electrode, with electrolysis performed at 0.6 V RHE (*i*R corrected). Inset shows the SEM images of the electrode after 16 h electrolysis which indicates retention of the nanosheet structure.

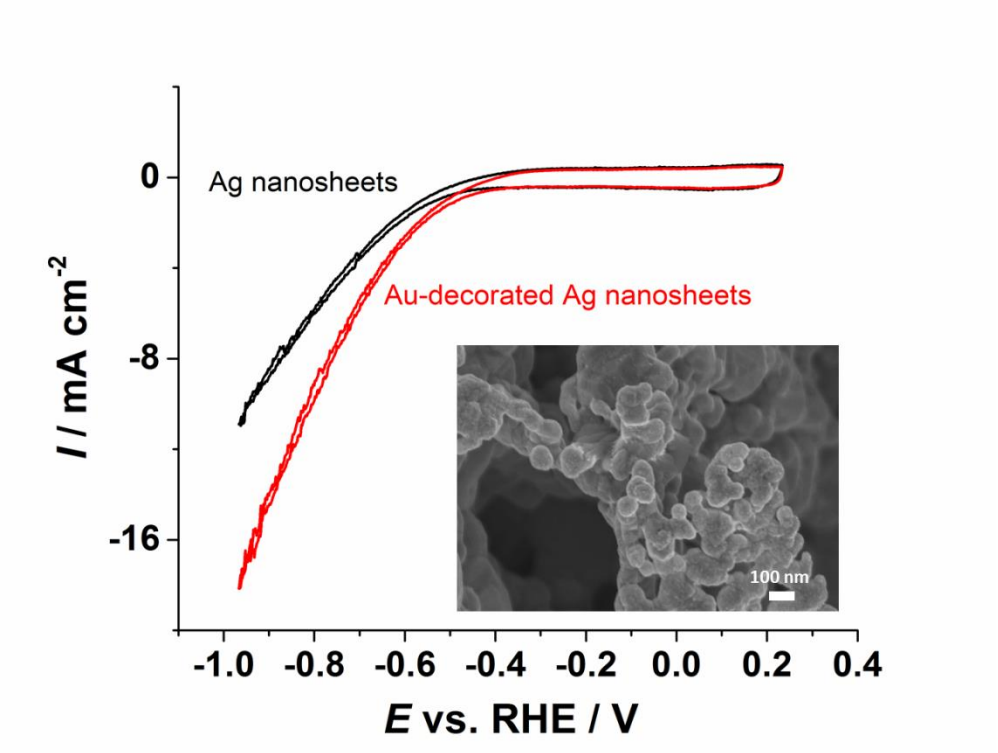

Figure S9. Comparison of cyclic voltammograms (*iR*-uncorrected) of unmodified Ag nanosheets (black curve) and Au-deposited Ag nanosheets (red curve) under electrocatalytic CO_2 reduction in 0.5 M $NaHCO_3$ electrolyte solution performed at a scan rate of 10 mV s^{-1}. Inset shows SEM image of Au deposited Ag nanosheets.

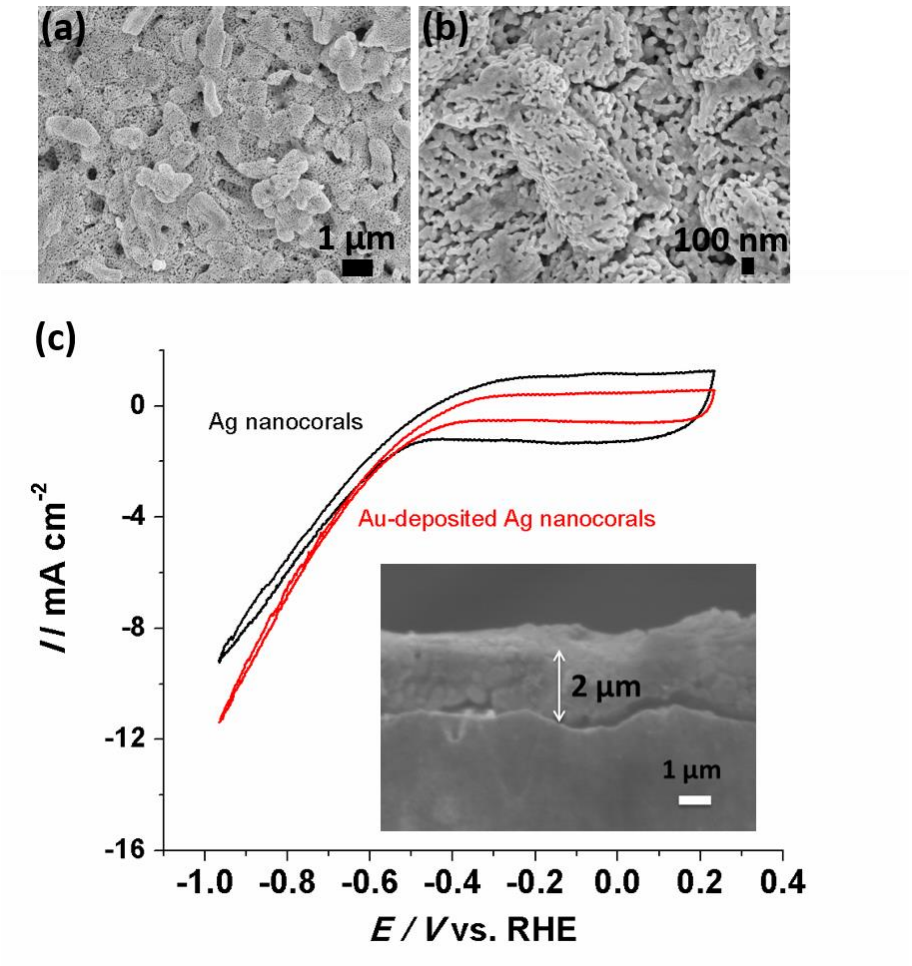

Figure S10 SEM images of Ag nanocorals obtained from: (a) electroreduced AgCl prepared in 1.0 M NaCl for 180s and (b) the higher magnification image; (c) Comparison of cyclic voltammograms (*i*R uncorrected) of the as-prepared reduced Ag nanocorals with (—) and without (—) gold deposited. The gold deposition was achieved by immersion in 0.5 mM $HAuCl_4$ aqueous solution for 60 s. Inset in (c) showing the cross-sectional Ag nanocorals.

References

1. Y. Zhao, C. Wang and G. G. Wallace, *J. Mater. Chem. A.* 2016, **4**, 10710.
2. Q. Lu, J. Rosen, Y. Zhou, G. S. Hutchings, Y. C. Kimmel, J. G. Chen and F. Jiao, *Nat. Commun.* 2014, **5**, 3242.
3. Y.-C. Hsieh, S. D. Senanayake, Y. Zhang, W. Xu and D. E. Polyansky, *ACS Catal.* 2015, **5**, 5349.
4. M. Ma, B. J. Trześniewski, J. Xie and W. A. Smith, *Angew. Chem.* 2016, **128**, 9900.
5. L. Zhang, Z. Wang, N. Mehio, X. Jin and S. Dai, *ChemSusChem.* 2016, **9**, 428.
6. Y. Yoon, A. S. Hall and Y. Surendranath, *Angew. Chem. Int. Ed.* 2016, **55**, 15282.
7. C. W. Li and M. W. Kanan, *J. Am. Chem. Soc.* 2012, **134**, 7231.
8. M. Asadi, B. Kumar, A. Behranginia, B. A. Rosen, A. Baskin, N. Repnin, D. Pisasale, P. Phillips, W. Zhu, R. Haasch, R. F. Klie, P. Král, J. Abiade and A. Salehi-Khojin, *Nat. Commun.* 2014, **5**, 4470.
9. Y. Chen, C. W. Li and M. W. Kanan, *J. Am. Chem. Soc.* 2012, **134**, 19969.